Journal of Electron Spectroscopy and Related Phenomena, 46 (1988) 55–84
Elsevier Science Publishers B.V., Amsterdam — Printed in The Netherlands

THE OSCILLATOR STRENGTHS FOR C1*s* AND O1*s* EXCITATION OF SOME SATURATED AND UNSATURATED ORGANIC ALCOHOLS, ACIDS AND ESTERS

I. ISHII and A.P. HITCHCOCK

Department of Chemistry, McMaster University, Hamilton, Ontario L8S 4M1 (Canada)

(Received 16 June 1987; in final form 10 August 1987)

ABSTRACT

Electron energy loss spectroscopy (ISEELS) under dipole scattering conditions is used to obtain the carbon and oxygen *K*-shell oscillator strength spectra of methanol (CH_3OH), propanol ($CH_3CH_2CH_2OH$), propenol ($CH_2{=}CHCH_2OH$), propargyl alcohol ($HC{\equiv}CCH_2OH$), propanoic acid (CH_3CH_2COOH), acrylic acid ($CH_2{=}CHCOOH$) and propiolic acid ($HC{\equiv}CCOOH$). A detailed interpretation of these spectra is presented, along with a comparison with the NEXAFS spectra of multilayers of these molecules adsorbed on a Si(1 1 1) surface, as recently reported by Outka et al. (Surf. Sci., 185 (1987) 53). Good agreement is found between the multilayer NEXAFS and the gas phase ISEEL spectra, except for the carboxylic acids which differ dramatically in the discrete portion of the O1*s* spectrum. Possible origins for this difference are discussed. The C1*s* and O1*s* spectra of methyl formate ($HCOOCH_3$) are also reported and interpreted in comparison with the spectra of formic acid and methanol.

INTRODUCTION

The probing of inner-shell excitation by electron energy loss (ISEELS) [1] or near edge X-ray absorption fine structure (NEXAFS) [2] techniques, provides a convenient means of exploring the unoccupied electronic structure of free or surface adsorbed molecules. Although the spectra of many simple, monofunctional species have been investigated [3], relatively few studies have been published of more complex, multi-functional molecules. In this work we report the first ISEELS studies of inner-shell excitation in three C_3 organic alcohols (propanol, propenol and propargyl), three C_3 organic acids (propanoic, acrylic and propiolic) and an ester (methyl formate). A major goal of this work was to test the concept of chromophores as applied to inner-shell excitations in the context of a recently developed correlation between $1s \rightarrow \sigma^*$ energies and intramolecular bond lengths [4]. If there is negligible interaction among the unsaturated C=O, C=C or C≡C chromophores in these molecules the spectra should resemble the sum of the spectra of the constituent groups. This idea is tested further by a comparison of the C1*s* and O1*s* spectra of the ester, $HCOOCH_3$, with those of the related acid (HCOOH) [5] and alcohol (CH_3OH) [6].

Outka et al. [7] have recently reported the C1*s* NEXAFS spectra of these C_3

0368-2048/88/$03.50

alcohols and the C1*s* and O1*s* NEXAFS of the C_3 acids condensed in multilayers (and in some cases, monolayers) on a Si(1 1 1) (7 × 7) surface. Although most of the NEXAFS and ISEEL spectra are very similar, characteristic, qualitative differences are observed between the present gas-phase O1*s* (but not C1*s*) results and the condensed phase NEXAFS spectra of the carboxylic acids. In previous comparisons of the spectra of benzene [8], cyclic hydrocarbons [9], thiophene [10], pyrrole [11, 12] and C_2 hydrocarbons [13, 14], the NEXAFS of multilayers has been found to be virtually identical to the gas phase ISEELS of the same species. Thus, the occurrence of a significant, qualitative difference in the O1*s* spectra of the condensed and vapor phases of all the carboxylic acids is a major observation of the present work. These differences suggest that changes in the electronic and/or geometric structure have occurred with condensation. A well-known effect is the dimerization of carboxylic acids in condensed phases and even in the gas phase under all but very low density conditions. Since the pressure in our sample chamber is very low ($< 10^{-4}$ torr) the spectra reported herein are those of the monomer. We discuss the possible geometric/electronic modifications which could explain the spectral changes with condensation.

EXPERIMENTAL

All of the inner-shell oscillator strength spectra reported herein were derived from electron energy loss spectra recorded using a final electron energy of 2.5 keV, a scattering angle of 2° and a FWHM resolution of 0.5 eV. These experimental conditions excite predominantly electric dipole transitions and thus the spectra can be quantitatively related to the soft X-ray photoabsorption spectra of these molecules. More detailed descriptions of the spectrometer [11, 15] and the experimental techniques [1] have been presented elsewhere. The species studied were high purity samples obtained from commercial sources. They were used without further purification except for freeze–pump–thaw degassing. The spectral energies were calibrated from the well-documented energies of sharp $1s \rightarrow \pi^*$ transitions in CO, CO_2 and O_2. In all cases, the calibration spectra were recorded by introducing the unknown and the calibrant through separate leak valves in order to ensure a constant gas mixture since the energy scale of our spectrometer was slightly sensitive to changes in the gas composition.

The oscillator strength spectra reported were obtained from the recorded energy loss spectra after the subtraction of a smooth curve fitted to the underlying, low intensity, valence ionization continuum (or the sum of the C1*s* and valence ionization continua in the case of the O1*s* spectra). This subtracted background is typically of the order of 5% of the intensity of the ($C1s^{-1}$, π^*) feature and 20% of the ($O1s^{-1}$, π^*) feature. The isolated core-excitation spectra were then converted to approximate absolute optical oscillator strengths (OS) by first, correcting for the kinematical differences between electron energy loss and photoabsorption (corresponding to a smooth upward tilt of 30% in the C1*s*

and 20% in the O1*s* spectral ranges shown), and second, normalizing the intensity at 25 eV above the IP to the calculated atomic oscillator strengths multiplied by the number of such atoms per molecule. At IP + 25 eV the calculated OS are 0.0077 and 0.0045 eV^{-1} for carbon and oxygen respectively [16]. We have recently presented a detailed rationale for this conversion procedure, demonstrated its accuracy and discussed its limitations [17].

RESULTS AND DISCUSSION

Alcohols

The oscillator strength spectra for the C1*s* and O1*s* excitation of the alcohols $CH_3CH_2CH_2OH$, $CH_2{=}CHCH_2OH$ and $HC{\equiv}CCH_2OH$ are shown in Figs. 1 and 2, respectively. The energies, term values and proposed assignments are summarized in Tables 1–3. Only the O1*s* IP of propanol was found in the

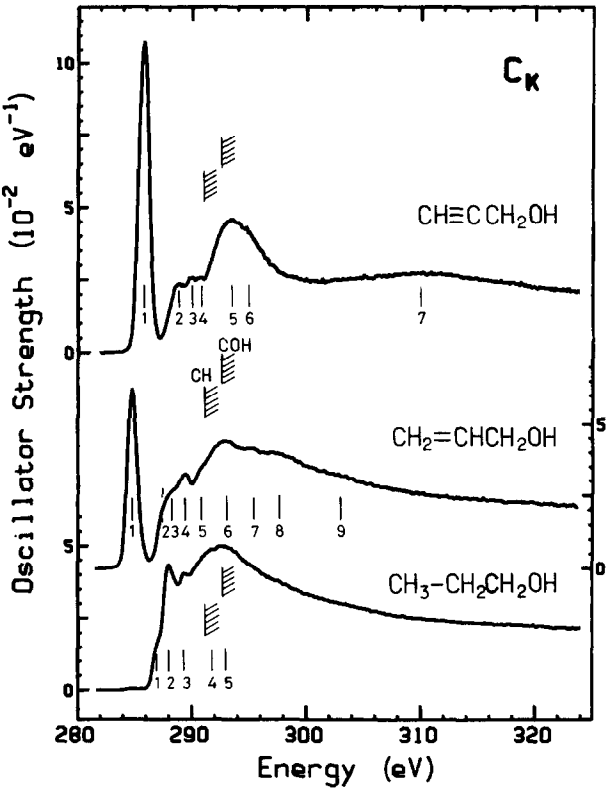

Fig. 1. Oscillator strengths for C1*s* excitation of propargyl alcohol, propenol and propanol derived from electron energy loss spectra (ISEELS) recorded with a final electron energy of 2.5 keV, an average scattering angle of 2° and a FWHM resolution of 0.6 eV. The spectra are plotted on common energy and intensity scales. The hatched lines indicate the location of the C1*s* IPs as estimated or measured by XPS.

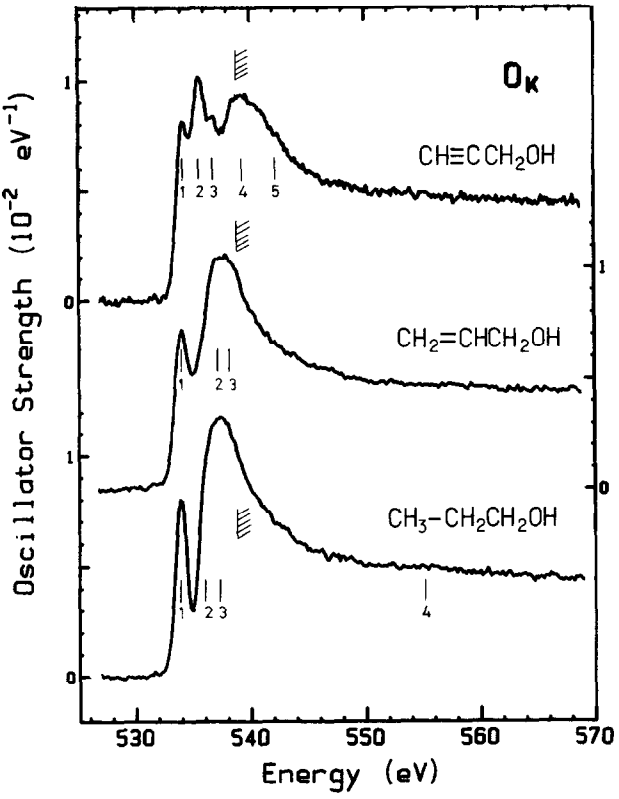

Fig. 2. Oscillator strengths for O1*s* excitation of propargyl alcohol, propenol and propanol derived from ISEELS. See caption to Fig. 1 for further details.

literature [18]. The other IPs were estimated as follows. Primary alcohols show a chemical shift only for the IP of the carbon to which the hydroxyl is attached ($CH_3C^*H_2OH$ — 292.5: CH_3OH — 292.5 eV). The more distant carbons have a typical hydrocarbon-like C1*s* IP ($C^*H_3CH_2OH$ — 291.1 eV). Thus, values of 291.0(3) and 292.5(3) eV are estimated for the CH_x and CH_2OH C1*s* IPs. The O1*s* IP of alcohols appears to decrease only slightly with increasing chain length (CH_3OH — 539.1; CH_3CH_2OH — 538.8; $CH_3CH_2CH_2OH$ — 538.8 eV) and thus a value of 538.8(3) eV was adopted for propenol and propargyl alcohol.

C1s spectra of C_3 alcohols

The C1*s* spectrum of propanol (Fig. 1) resembles that of other saturated hydrocarbons [13, 19] in that the discrete region exhibits a relatively strong, sharp feature attributed to excitations of C1*s* to $3p/\pi^*$(C—H), a mixed Rydberg/valence orbital with σ^*(C—H) valence character [19]. Bands observed at similar energies in the NEXAFS of hydrocarbon monolayers on metal surfaces

TABLE 1

Absolute energies, term values and proposed assignments for features in the C1*s* and O1*s* spectra of propanol

Carbon 1*s*							Oxygen 1*s*			
Feature	Energy (eV)		Term value (eV)		Assignment		Feature	Energy (eV)	Term value (eV)	Assignment
	Solid [7]	Gas	$T_{CH_3CH_2}$	T_{CH_2OH}	CH_3CH_2	CH_2OH				
1		287.0	4.0	5.5	3*s*	σ^*(O—H)	1	533.9[a]	4.9	σ^*(O—H)
2		288.0[a]	3.0	4.5	3*p*/π^*(C—H)	3*s*	2 (sh)	536.0	2.8	3*p*
3	289.4	289.3	1.7	3.2	Ryd.	3*p*/π^*(C—H)	3	537.2	1.6	σ^*(C—O)
IP(CH_x)		291.0(3)[b]					IP	538.8[c]		
4		291.6	−0.6	–	σ^*(C—C)	–	4	555(1)	−11	Double excitation?
IP(CH_2OH)		292.5(3)[b]								
5	293	292.7	–	−0.2	–	σ^*(C—O)				

[a] Calibration: C1*s*, 2.70(5) eV below ($C1s^{-1}$, π^*) of CO_2 (290.74(5) eV [19]); O1*s*, 3.08(5) eV below ($O1s^{-1}$, π^*) of O_2 (530.8(1) eV [39]). [b] C1*s* IPs (estimated, see text). [c] O1*s* IP from XPS [18].

TABLE 2

Absolute energies, term values and proposed assignments for features in the C1*s* and O1*s* spectra of propenol

Carbon 1*s*							Oxygen 1*s*			
Feature	Energy (eV)		Term value (eV)		Assignment		Feature	Energy (eV)	Term value (eV)	Assignment
	Solid [7]	Gas	T_{CH_2CH}	T_{CH_2OH}	CH_2CH	CH_2OH				
1	285.0	284.8[a]	6.2	–	π^*(C=C)		1	533.9[a]	4.9	σ^*(O—H)
2		287.4	–	5.1	–	3*s*	2 (sh)	537.0	1.8	Ryd.
3		288.4	2.6	–	3*p*/π^*(C—H)	–	3	538.0	0.8	σ^*(C—O)
4	289.4	289.4	1.6	3.1	4*p*	3*p*/π^*(C—H)	IP	538.8[b]		
5		290.8	–	1.7	–	4*p*				
IP(CH_x)		291.0(3)[b]								
IP(CH_2OH)		292.5(3)[b]								
6	293	292.8	−1.8	−0.3	σ^*(C—C)	σ^*(C—O)				
7		295.3	–	−2.8	–	σ^*(C—C)				
8	300	297.7	−6.6	–	σ^*(C=C)	–				
9		303(2)	–	−10	–	σ^*(C=C)				

[a] Calibration: C1*s*, 2.61(5) eV below ($C1s^{-1}$, π^*) of CO (287.40(2) eV [40]); O1*s*, 3.14(5) eV below ($O1s^{-1}$, π^*) of O_2. [b] IPs (estimated, see text).

TABLE 3

Absolute energies, term values and proposed assignments for features in the C1s and O1s spectra of propargyl alcohol

Carbon 1s							Oxygen 1s			
Feature	Energy (eV)		Term value (eV)		Assignment		Feature	Energy (eV)	Term value (eV)	Assignment
	Solid [7]	Gas	$T_{HC\equiv C}$	T_{CH_2OH}	$HC\equiv C$	CH_2OH				
1	285.7	285.8[a]	5.4	–	$\pi^*(C\equiv C)$		1	534.1	4.7	$\sigma^*(O—H)$
2		288.9	2.3	3.6	$3p/\pi^*(C—H)$	3s	2	535.6[a]	3.2	3p (possibly impurity)
3	289.2	290.0	1.2	2.5	Ryd.	$3p/\pi^*(C—H)$	3	536.8	0.8	Ryd. (possibly impurity)
4		290.7	–	1.8	–	Ryd.	IP	538.8(2)[b]		
IP($HC\equiv C$)		291.0(3)[b]					4	539.2	−0.4	$\sigma^*(C—O)$
IP(CH_2OH)		292.5(3)[b]					5	542(2)	−3	$2e^-$ or $\sigma^*(C—C)$
5	293	293.4	−2.2	−0.9	$\sigma^*(C—C)$	$\sigma^*(C—O)$				
6		295(1)	–	−3	–	$\sigma^*(C—C)$				
7	310	310	−19	–	$\sigma^*(C\equiv C)$	–				

[a] Calibration: C1s, 1.56(5) eV below ($C1s^{-1}$, π^*) of CO; O1s, 4.77(5) eV above ($O1s^{-1}$, π^*) of O_2. [b] IPs (estimated, see text).

have been identified on the basis of their polarization dependence as C1*s* excitations to orbitals with a dominant σ^*(C—H) character [20]. As in the gas phase spectra of other hydrocarbons [19], this band has a low-energy shoulder assigned to C1*s* → 3*s* Rydberg transitions. The structured, discrete region of the spectrum is somewhat wider than that of a simple hydrocarbon since there are two C1*s* ionization limits separated by 1.5 eV. The main feature of the spectrum is a broad maximum in the region of the IPs, which is attributed to σ^*(C—C) and σ^*(C—O) resonances.

The C1*s* spectrum of propenol differs dramatically from that of propanol because of the addition of an intense, low-lying C1*s* → π^*(C=C) transition. Its energy (284.8 eV) is essentially the same as that in the monofunctional prototype, ethene (284.7 eV) [13], indicating that there is little interaction with the hydroxyl group. Thus there appears to be a good separation between the π and σ manifolds in this molecule. A strong σ^*(C—C)/σ^*(C—O) resonance maximum is observed as in propanol while the features attributed to C1*s* → 3*p*/π^*(C—H) transitions are somewhat weaker, consistent with the reduced number of C—H bonds. Although a σ^*(C=C) resonance is expected around 300 eV [4] this is not well defined. However, there is additional intensity above 294 eV in propenol as compared to propanol. The σ^*(C=C) resonance in ethene is also weak [4] but it has been clearly identified as the broad feature at 300 eV in the gas phase spectrum [17] via the polarization dependence of the corresponding feature in the NEXAFS spectra of ethene adsorbed on inert metals [14].

The C1*s* spectrum of propargyl alcohol exhibits a strong, low-lying C1*s* → π^*(C≡C) transition which is approximately twice as intense as that in propenol. Its energy is 1 eV higher than that in propenol, paralleling the difference between the transition in ethene and ethyne [13]. The Rydberg/π^*(C—H) region below the IP is notably weaker (relative to the σ^*(C—C)/σ^*(C—O) resonance or the continuum) than in the other two alcohols, which is consistent with the further reduction in the number of C—H bonds. The σ^*(C≡C) resonance is the well defined broad feature around 310 eV, at a position similar to that found in ethyne [4], propyne [21] and 2-butyne [22]. Both the π^* and σ^* features associated with the C≡C group appear to have very characteristic term values and intensities.

The solid phase NEXAFS spectrum [7] of each of these species is remarkably similar to the corresponding gas phase spectra indicating that there is negligible intermolecular interaction within the multilayers. This is further evidenced by the absence of any polarization dependence of the NEXAFS spectra [7] which indicates a random orientation and thus no tendency for molecular alignment during the formation of the multilayer, such as occurs if there are strong, directional intermolecular interactions.

O1s spectra of C_3 alcohols

The O1*s* spectra of all three alcohols (Fig. 2) are dominated by σ^*(O—H) and σ^*(C—O) resonances. The O1*s* → σ^*(C—O) transition occurs at a somewhat

higher term value than the C1*s* → σ^*(C—C)/σ^*(C—O) resonance because of the minimal contribution from O1*s* → σ^*(C—C) and the fact that the 1*s* → σ^*(C—O) energy is intrinsically lower than 1*s* → σ^*(C—C) energy, which is consistent with the observed *Z*-dependence of the σ^* term values [4]. The well resolved low-lying peak at 533.9 eV in propanol is assigned to O1*s* → σ^*(O—H) transitions. Corresponding features occur in the O1*s* spectra of all alcohols studied to date [6, 23].

The O1*s* spectrum of propenol is quite similar to that of propanol, illustrating once again that inner-shell excitation is sensitive predominantly to the unoccupied electronic structure in the immediate vicinity of the core-excited atom. Thus, O1*s* excitations to π^*(C=C) or σ^*(C=C) do not appear in the O1*s* spectrum of propenol or acrylic acid while O1*s* excitations to π^*(C≡C) or

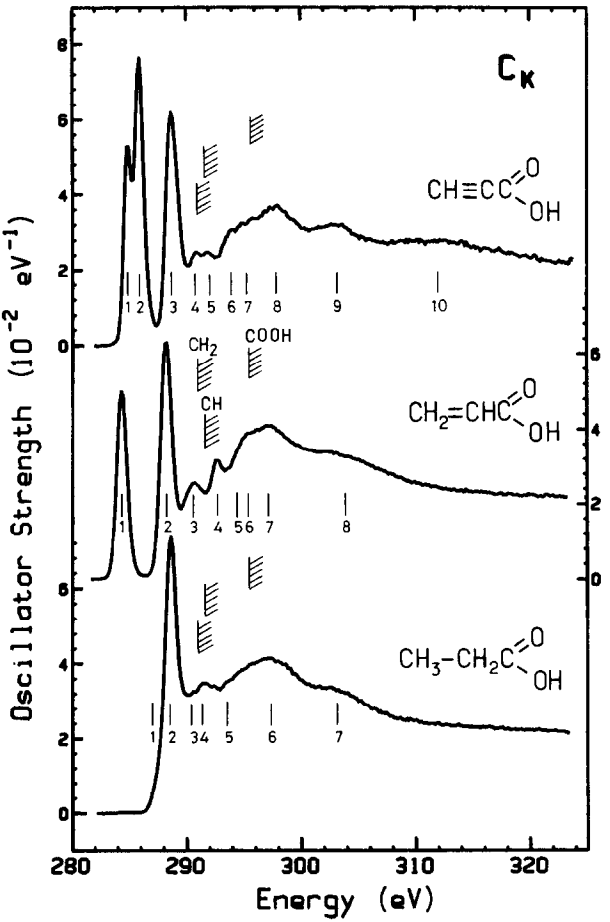

Fig. 3. Oscillator strengths for C1*s* excitation of propiolic, acrylic and propanoic acid derived from ISEELS. See caption to Fig. 1 for further details.

σ^*(C≡C) are not observed in propynol or propiolic acid. The feature attributed to σ^*(O—H) is also well resolved in propenol, although there is some shift to higher energy relative to that in propanol. This trend continues in propargyl alcohol so that the O1*s* → σ^*(O—H) transition is not such a prominent feature, even though feature 1 in the propargyl alcohol spectrum is of similar intensity to the σ^*(O—H) feature in that of the other two alcohols. The $HC{\equiv}CCH_2OH$ spectrum differs further in that two additional features are observed in the discrete region between the σ^*(O—H) and σ^*(C—O) resonances. It is possible that these features (2 and 3) arise from impurities although they do not match any recorded features of molecules and the mass spectrum of the sample (recorded simultaneously) gave no evidence of the presence of other species. They are tentatively assigned as Rydberg features.

The O1*s* NEXAFS spectra of the alcohol multilayers were not reported by Outka et al. [7]. Had these been available the valence or Rydberg character of the discrete line attributed to σ^*(O—H) could have been investigated. If our σ^*(O—H) assignment is correct, a NEXAFS feature should exist at 534 eV in those cases where the hydroxyl hydrogen is not lost upon chemisorption. In previous NEXAFS studies of monolayers of CH_3OH on Cu(100) [24] and Cu(110) [25], a 534 eV peak was not observed, which is consistent with the assumed methoxy structure in each case. Very recently, Crapper et al. [26] reported the O1*s* NEXAFS of samples in which both ethanol and ethoxy are believed to be co-adsorbed on Cu(110). A shoulder at 534(1) eV, observed in all spectra, could arise from the proposed excitation to the ($O1s^{-1}$, σ^*(O—H)) state in ethanol. The absence of any polarization dependence of this feature would then indicate that the O—H bond direction is randomly oriented with respect to the surface. Crapper et al. [26] proposed that this feature is related to levels associated with binding to the Cu substrate and thus further studies are required to clarify its origin. If σ^*(O—H) resonances persist in the NEXAFS of surface adsorbates, they could provide a useful means of following the reactions of hydroxyl compounds, such as the conversion between alcohol and alkoxy species, on surfaces.

Carboxylic acids

The oscillator strength spectra for the C1*s* and O1*s* excitation of the carboxylic acids CH_3CH_2COOH, $CH_2{=}CHCOOH$ and $HC{\equiv}CCOOH$ are shown in Fig. 3 (C1*s*) and Fig. 4 (O1*s*). The energies, term values and proposed assignments are listed in Tables 4–6. Since the IPs of the C_3 carboxylic acids have not been measured by XPS, we have estimated them as follows: the IP of the carboxyl carbon is strongly shifted by the two attached oxygens — the C1*s*(COOH) IPs of formic acid and acetic acid are 295.8 and 295.3 eV, respectively [18]. Based on these values we estimate a C1*s*(COOH) IP of 295.5(3) eV in the C_3 acids. In contrast to the C_3 alcohols, the IPs of the carbon adjacent to the carboxyl carbon (CH_2 in propanoic, CH in acrylic and —C≡ in propiolic acid) probably differ significantly from that of the more distant carbon. This is

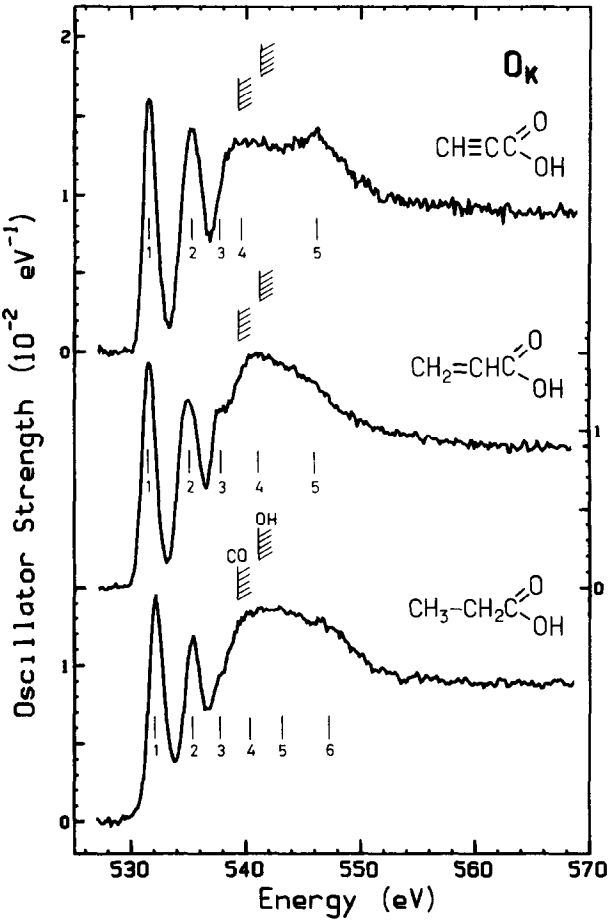

Fig. 4. Oscillator strengths for O1*s* excitation of propiolic, acrylic and propanoic acid derived from ISEELS. See caption to Fig. 1 for further details.

suggested by the C1*s*(CH_3) IP of acetic acid (291.6 eV) which is almost 1 eV higher than that of a typical hydrocarbon. Thus we estimate that the carbons adjacent to the COOH group have an IP of 291.5(5) eV. The carbon furthest from the carboxyl group will have an IP around 291.0(3) eV, closer to that of a typical hydrocarbon. The O1*s* IPs of formic (C=O — 539.0, OH — 540.6 eV) and acetic acid (C=O — 539.2, OH — 541.0 eV) have been used to estimate O1*s* IPs of 539.2(3) eV for the O1*s*(C=O) and 541.0(3) eV for the O1*s*(OH) for the C_3 acids. The uncertainty in the IPs is a considerable limitation to our spectral interpretation. It would have been very helpful to have had the XPS spectra of these species.

TABLE 4

Absolute energies, term values and proposed assignments for features in the C1*s* and O1*s* spectra of propanoic acid

Carbon 1*s*									Oxygen 1*s*						
Feature	Energy (eV)		Term value (eV)			Assignment			Feature	Energy (eV)		*T* (eV)		Assignment	
	Solid [7]	Gas	T_{CH_3}	T_{CH_2}	T_{CO_2H}	CH_3	CH_2	CO_2H		Solid [7]	Gas	C=O	OH	C=O	OH
1		287.2	3.8	4.3	–	3*s*	3*s*	–	1	(532.8)	532.1[a]	7 1	–	π^*(C=O)	–
2	288.5	288.5[a]	2.5	3 0	7.0	3*p*/π^*(C—H)	3*p*/π^*(C—H)	π^*(C=O)	2		535.4	3 8	5.6	3*s*	π^*(C=O)
3		290.2	–	1.3	–	–	4*p*	–	3		537.7	1.5	3.3	4*p*	3*p*/σ^*(O—H)
IP(CH_3)		291.0(3)[b]							IP(C=O)		539.2(3)[b]				
4	291	291.3	– 0 3	–	4.2	σ^*(C—C)	–	3*s*	IP(OH)		541.0(3)[b]				
IP(CH_2)		291.5(5)[b]							4	540.1	540.2	– 1.0		σ^*(C—O)	–
5	292.5	293.3	–	– 1.0	2 2	–	σ^*(C—C)	3*p*	5		543(1)	–	– 2.0		σ^*(C—O)
IP(CO_2H)		295.5(3)[b]							6	544.4	547(2)	– 8	–	σ^*(C=O)	–
6	297	297(1)	–	– 5.5	– 1.5	–	σ^*(C=O)	σ^*(C—O)							
7	301	303(2)	–	–	– 8	–	–	σ^*(C=O)							

[a] Calibration. C1*s*, 2.29(5) eV below ($C1s^{-1}$, π^*) of CO_2; O1*s*, 3 25(5) eV below ($O1s^{-1}$, π^*) of CO_2 (535.4(1) eV [41]) [b] IPs (estimated, see text).

TABLE 5

Absolute energies, term values and proposed assignments for features in the C1*s* and O1*s* spectra of acrylic acid

Carbon 1*s*									Oxygen 1*s*						
Feature	Energy (eV)		Term value (eV)			Assignment			Feature	Energy (eV)		Term value (eV)		Assignment	
	Solid [7]	Gas	T_{CH_2}	T_{CH}	T_{CO_2H}	CH_2	CH	CO_2H		Solid [7]	Gas	C=O	OH	C=O	OH
1	284.4	284.3	6 7	7.2	–	π^*(C=C)	π^*(C=C)	–	1	(532.8)	531.5[a]	7.7	–	π^*(C=O)	–
2	288.5	288.2[a]	2 8	3.3	7 3	3*p*/π^*(C—H)	3*p*/π^*(C—H)	π^*(C=O)	2		535.1	4.1	5.9	3*s*	π^*(C=O)
3	290 3	290.6	–	0.9	4.9	–	Ryd.	3*s*	3		537.9	1.3	3.1	Ryd.	3*p*/σ^*(O—H)
IP(CH_2)		291.0(3)[b]							IP(C=O)		539.2(3)[b]				
IP(CH)		291.5(5)[b]							IP(OH)		541.0(3)[b]				
4	293.0	292.6	– 1.6	– 1 1	2.9	σ^*(C—C)	σ^*(C—C)	3*p*/π^*(C—H)	4	540.1	541(1)	–	0	–	σ^*(C—O)
5		294.5	–	– 3.0	1.0	–	σ^*(C—O)	4*p*	5	544 4	546(2)	– 7	–	σ^*(C=O)	–
IP(CO_2H)		295.5(3)[b]													
6		295.6	–	–	– 0 1	–	–	σ^*(C—C)							
7	297	297(1)	–	–	– 2	–	–	σ^*(C—O)							
8	302	304(1)	– 13	– 12	– 9	σ^*(C=C)	σ^*(C=C)	σ^*(C=O)							

[a] Calibration: C1*s*, 2.54(5) eV below (C1s^{-1}, π^*) of CO_2; O1*s*, 3.89(5) eV below (O1s^{-1}, π^*) of CO_2 [b] IPs (estimated, see text).

TABLE 6

Absolute energies, term values and proposed assignments for features in the C1*s* and O1*s* spectra of propiolic acid

Carbon 1*s*									Oxygen 1*s*						
Feature	Energy (eV)		Term value (eV)			Assignment			Feature	Energy (eV)		Term value (eV)		Assignment	
	Solid [7]	Gas	T_{CH}	$T_{C\equiv}$	T_{CO_2H}	CH	C≡	CO_2H		Solid [7]	Gas	C=O	OH	C=O	OH
1	284.8	284 9	6 1	(6 6)	–	π^*(C≡C)	π^*(C≡C)	–	1	(537 7)	531 5[a]	7.7	–	π^*(C=O)	–
2	286.0	285 9[a]	5.1	5.6	–	π^*(C≡C)	π^*(C≡C)	–	2		535.2	4.0	5.8	3*s*	π^*(C=O)
3	288.6	288.9	2.1	2.6	6 6	3*p*/π^*(C—H)	3*p*/π^*(C—H)	π^*(C=O)	3 sh		537 8	1.4	3 2	Ryd.	3*p*/σ^*(O—H)
4		290.8	0.2	0.7	4.7	Ryd	Ryd.	3*s*	IP(C=O)		539.2(3)[b]				
IP(CH)		291.0(3)[b]							4	540 2	539.5(5)	– 0.3	1.5	σ^*(C—O)	σ^*(C—O)
IP(C≡C)		291 5(5)[b]							IP(OH)		541.0(3)[b]				
5		292.1	– 1.1	–	3 4	σ^*(C—C)	–	3*p*	5	544.8	546 0(5)	– 6.8	–	σ^*(C=O)	
6		293 9	–	– 2.4	1.6	–	σ^*(C—C)	4*p*							
7	295	294.8	–	–	0.7	–	–	Ryd.							
IP(CO_2H)		295.5(3)[b]													
8		297.8	–	– 6.3	– 2.3	–	σ^*(C—O)	σ^*(C—O)							
9	304	303(1)	–	–	– 8	–	–	σ^*(C=O)							
10	312.5	312(2)	– 21	– 20	–	σ^*(C≡C)	σ^*(C≡C)	–							

[a] Calibration: C1*s*, 4.86(4) eV below (C1s^{-1}, π^*) of CO_2, O1*s*, 3.89(5) eV below (O1s^{-1}, π^*) of CO_2. [b] IPs (estimated, see text)

C1s spectra of C_3 acids

The C1*s* spectrum of propanoic acid (Fig. 3) is similar to that of propanol except for the intense C1*s*(COOH) → π^*(C=O) transition (feature 1) at 288.5 eV (T = 7.0 eV) superimposed on the structure below the C1*s*(CH_x) IPs and the additional continuum structure at 303 eV (feature 7). There is a shoulder (287.2 eV) on the low energy side of the π^*(C=O) feature which is assigned to C1*s*(CH_x) → 3*s* transitions, based on its term value and similarity to the corresponding feature in propanol. The broad maxima (6 and 7) in the continuum are attributed to the σ^*(C—O) and σ^*(C=O) resonances. Similar features are observed in the C1*s* spectra of all three carboxylic acids as well as that of formic acid [5]. Peak 4, at 291.3 eV, is attributed to the overlap between the broad C1*s*(CH_x) → σ^*(C—C) resonance and the sharper C1*s*(COOH) → 3*s* transition. Although C1*s*(CH_x) → 3*p*/π^*(C—H) transitions are fairly prominent in the alcohol spectra, their counterparts in those of the acids are less clear because of the greater spectral congestion associated with transitions leading to three ionization limits separated by several eV. They probably occur at about the same energy as the much more intense 1*s*(COOH) → π^*(C=O) transitions.

The C1*s* spectrum of acrylic acid differs from that of propanoic acid chiefly by the addition of the C1*s*(CH_x) → π^*(C=C) transition at 284.3 eV ($T(CH_2)$ = 6.7, T(CH) = 7.2 eV). Although we estimate that the C1*s*(CH_2) and C1*s*(CH) IPs are separated by 0.5 eV, only one symmetric π^*(C=C) feature is detected which has a FWHM of 1.1 eV. The 1*s* → π^* transition in ethene exhibits a high energy shoulder at our experimental resolution [17], which corresponds to a resolvable ν(C—H) vibrational band at high resolution [13]. Ab initio calculations for the ($C1s^{-1}$, π^*) state of ethene [27] indicate that the excitation of ν(C—H) results from the change in the effective core charge rather than any specific σ^*(C—H) character of the π^*(C=C) orbital, thus a similar vibrational excitation is expected in acrylic acid and propenol. The C1*s* → π^*(C=C) transition in propenol is detectably asymmetric and narrower (0.9 eV FWHM) than that in acrylic acid. The symmetrization and broadening of the π^*(C=C) peak in acrylic acid is thus probably related to the presence of roughly equal contributions from C1*s*(CH_2) → π^*(C=C) and C1*s*(CH) → π^*(C=C) transitions.

The oscillator strength of the π^*(C=C) feature in acrylic acid is slightly less than that of the π^*(C=O) feature, which at first impression is somewhat surprising since two C1*s*(CH_x) → π^*(C=C) transitions contribute to peak 1 whereas the second peak results from excitations to the π^*(C=O) orbital from only a single C1*s*(COOH) orbital. This indicates, on a per-transition basis, that C1*s* → π^*(C=O) transitions are somewhat more than twice as intense as C1*s* → π^*(C=C) transitions. This observation is consistent with recent measurements of the 1*s* → π^*(C=C) oscillator strength in ethene (0.034 per carbon atom [17]) and the 1*s* → π^*(C=O) oscillator strength in HCOX compounds ($HCONH_2$ — 0.074, HCOOH — 0.080, HCOF — 0.104 [5]). The C1*s*(CH_x) → π^*(C=C) oscillator strength in propenol (0.066) and acrylic acid (0.055) are

similar, further supporting our interpretation that both C1s(CH_x) → π^*(C=C) transitions contribute to the 284.3 eV peak. The π^* oscillator strengths are summarized in Tables 8 and 9 and discussed in further detail later.

The C1s(COOH) continuum of acrylic acid (Fig. 3) exhibits the σ^*(C—C), σ^*(C—O) and σ^*(C=O) resonances common to all the carboxylic acids. The region around the C1s(CH_x) IPs is more sharply structured in acrylic acid than in propanoic acid, consistent with reduced contributions from C1s(CH_x) → σ^*(C—C). As with propenol, the C1s → σ^*(C=C) resonance expected around 301–302 eV is not directly evident. However, feature 8 at 303 eV in acrylic acid is somewhat broader than the corresponding σ^*(C=O) features in the other two acids, which we interpret as indirect evidence for the σ^*(C=C).

The C1s spectrum of propiolic acid contains C1s(COOH) → π^*(C=O), σ^*(C—O) and σ^*(C=O) features at similar energies to those in the spectra of the other two acids. The C1s(CH_x) → σ^*(C≡C) resonance is clearly observed as a broad maximum around 312 eV, as in propargyl alcohol and all other alkynes. However, the C1s → π^*(C≡C) region differs dramatically from that of ethyne [13] or propargyl alcohol (Fig. 1) in that two sharp peaks are observed rather than a single one due to the C1s(C≡) → π^*(C≡C) transition. One could speculate that these correspond to C1s(CH) → π^*(C≡C) and C1s(C≡) → π^*(C≡C) transitions. However, the separation of the two peaks (1.06(3) eV) is approximately twice that of our estimated IPs (0.5 eV). In addition, if this explanation was correct one would expect a visible doubling of the π^*(C=C) peak in acrylic acid, which is not observed. The NEXAFS of multilayer propiolic acid also indicates that the splitting of the C1s energies is not the correct interpretation since two π^*(C≡C) peaks are observed and, furthermore, they exhibit opposite polarization dependences. As Outka et al. [7] have explained, the splitting arises from the conjugation of the π^*(C=O) with the component of the π^*(C≡C) orbital that is in the same plane (see Figs. 6 and 7 of ref. 7). Comparison of term values with those of propargyl alcohol ($T(\pi^*(C{\equiv}C))$ = 5.4 eV) indicates that the second peak in propiolic acid (T(CH) = 5.1 eV, T(C≡C) = 5.6 eV) corresponds to C1s(CH_x) → π^*(C≡C) transitions, the essentially unmodified component, while it is the first peak (T(CH) = 6.1 eV, T(C≡) = 6.6 eV) which arises from C1s(CH_x) excitation to $\pi^{*\prime}$(C≡C), the conjugated component of the π^*(C≡C) orbital. The NEXAFS polarization dependence of these two peaks is consistent with this interpretation [7].

As noted in a previous analysis of the multilayer NEXAFS [7], the downward shift of 0.9 eV in the C1s(CH_x) → π^*(C≡C) transition caused by the conjugation is accompanied by a simultaneous shift upward, of 0.6 eV, in the C1s(C=O) → π^*(C=O) transition (based on comparison of propiolic to both propanoic and acrylic acid). The inequality of these shifts suggests that one needs to consider both the π and π^* orbital interactions in order to preserve the center of gravity in the interaction. If this is so, there should be different shifts in the unperturbed vs. the conjugated π(C=O) and π(C≡C) orbital energies as

measured by PES. Klapstein [28] has recently examined the effects of conjugation on the orbital energies of a series of α,β-unsaturated species. Comparison of the PES of propiolic acid [28] with those of propynol [28] and formic acid [29] indicates that the π'(C≡C) IP shifts downwards (i.e. to higher binding energy) by 0.5 eV while the π(C=O) IP shifts upwards by 0.9 eV. Although the π^* orbital energies will be disturbed from those of the ground state because of the C1*s* core hole, this comparison suggests that there is some compensation between the occupied and unoccupied manifolds in the shifts associated with π(C≡C) and π(C=O) conjugation. It appears that in the unoccupied manifold it is the π^*(C=C) orbital which is most affected by the conjugation, while in the occupied manifold the π(C=O) orbital is shifted to the greater extent.

Another effect of this conjugation should be a shortening of the C—COOH bond. Although the geometry of propiolic acid has not been determined by electron diffraction, the same contraction due to conjugation should occur in propynal (HC≡C—CHO). The C—C bond in propynal is 1.45 Å [30], considerably shorter than a normal C—C bond of 1.50 Å (although not much shorter than the C—C bond in propyne (1.458 Å) or 2-butyne (1.468 Å) [30], where the C—C bond lengths are reduced by hyperconjugation). According to the bond length correlation [4], the reduced C—C bond length should be signaled by a shift of the C1*s*(COOH) → σ^*(C—C) transition to higher energy. This is consistent with the increase of ca. 1 eV in the energy of feature 8 in propiolic acid (principally C1*s*(COOH) → σ^*(C—O)) as compared to its counterpart in the C1*s* spectra of the other two acids (features 7 in acrylic and 6 in propanoic acid).

The C1*s* NEXAFS of the C_3 carboxylic acids [7] are in excellent agreement with the present results, indicating that the effects of intermolecular interaction are minimal in the region of the carbon atoms. In general, the energies of the C1*s* → π^*(C=O) transitions are 0.3–0.4 eV lower in the solid than in the gas phase whereas the π^*(C=C) and π^*(C≡C) features agree within 0.1 eV. Although these shifts are at the limits of reliability because of uncertainties in the NEXAFS calibration, they suggest modifications in the carboxyl region of the solid through dimerization and/or possibly deprotonation, as is evidenced clearly in the O1*s* spectra and discussed in detail below. Neither acrylic or propanoic acid exhibited polarization dependence in the multilayer, indicating random orientation and largely non-directional intermolecular interactions. However, the NEXAFS of the propiolic acid multilayer exhibited polarization consistent with our spectral assignments. An average tilt of 37° between the molecular and the surface planes was deduced from a detailed study of the π^* polarization dependence [7].

O1s spectra of C_3 acids

The O1*s* spectra of the three carboxylic acids in the gas phase (Fig. 4) are all very similar to each other and to that of formic acid [5] (Fig. 5), indicating that the O1*s* spectra are only sensitive to the unoccupied electronic structure in the

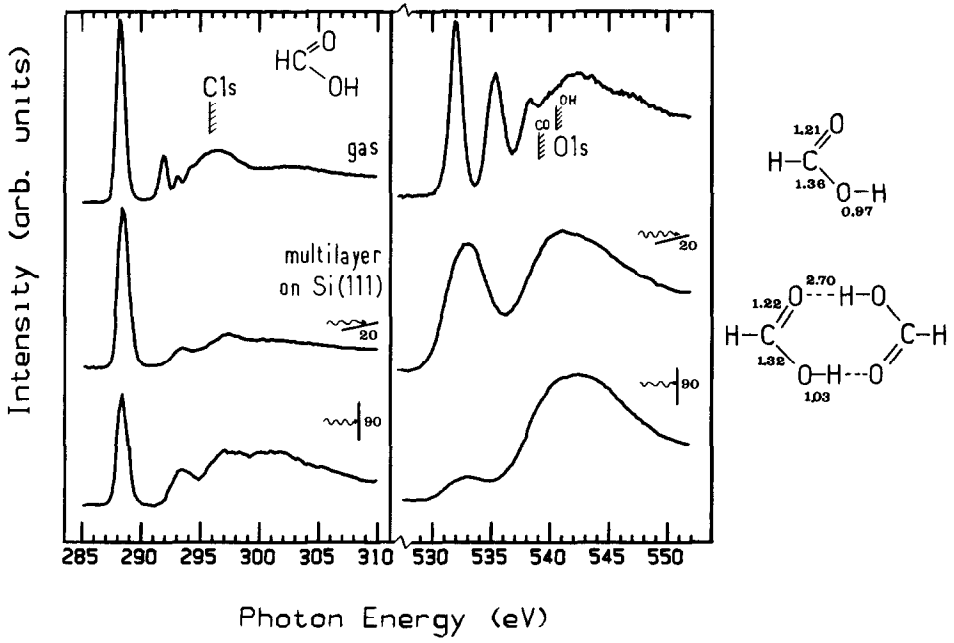

Fig. 5. Comparison of the C1*s* and O1*s* ISEEL spectra of formic acid vapor with the corresponding NEXAFS spectra of a multilayer of formic acid on Si(1 1 1) (7 × 7). The geometries of the formic acid monomer and dimer in the gas phase, as determined by electron diffraction [30] are also shown.

immediate vicinity of the oxygen atoms. The O1*s*(C=O) → π^*(C=O) transitions (feature 1 in each spectrum) occur at essentially the same energy in all three carboxylic acids. Thus it appears that this transition is not appreciably modified by the interaction between the π^*(C=O) and the carbon–carbon unsaturated centres, even in propiolic acid where the conjugation of the π^*(C=O) and the $\pi^{*\prime}$(C≡C) orbitals produced dramatic changes in the C1*s* spectrum and a detectable shift in the C1*s*(C=O) → π^*(C=O) transition relative to that in acrylic acid. In view of the delocalization of the π^*(C=O) and $\pi^{*\prime}$(C≡C) orbitals it is somewhat surprising that an O1*s*(C=O) → $\pi^{*\prime}$(C≡C) transition is not resolved. Such a charge transfer transition would be expected to have a term value somewhat smaller than that for the C1*s* → $\pi^{*\prime}$(C≡C) transition. These transitions may contribute to feature 2 in the O1*s* spectrum of propiolic acid (Fig. 4). This feature is believed to be predominantly O1*s*(O—H) → π^*(C=O) (see the following section) but it is clearly broader and more intense than the corresponding feature in the other C_3 acids.

As with formic acid [5], a strong, well-isolated second feature is observed in each O1*s* spectrum which is attributed primarily to the charge transfer transition, O1*s*(OH) → π^*(C=O). The intensity of this feature is rather surprising since C1*s*(CH_3) → π^*(C=O) transitions are absent, or at most very weak, in the spectra of acetone and acetaldehyde [31]. However, the existence

of prominent X1*s* → π^*(C=O) transitions in the N1*s* spectrum of formamide and the F1*s* spectrum of formyl fluoride [5] supports our interpretation. Even more surprising is the apparently complete absence of this feature in the O1*s* NEXAFS of multilayers of these acids [7]. Rationalizations for this are discussed in the following section. With regard to the other spectral features, the O1*s* continua exhibit broad σ^*(C—O) and σ^*(C=O) resonances similar to those observed in the C1*s* spectra (Fig. 3). O1*s* → Rydberg transitions appear to be rather weak in the acids, as in the alcohols. Feature 3 at ~538 eV, is attributed to the overlap of O1*s*(C=O) → Rydberg and O1*s*(OH) → σ^*(O—H) transitions. Thus this feature is believed to correspond in part to the first feature in the O1*s* spectra of the alcohols, although with this assignment the σ^*(O—H) term value in the acids (3.1–3.4 eV) is somewhat smaller than that in the alcohols (4.7–4.9 eV).

Comparison with the O1s NEXAFS of carboxylic acid multilayers

NEXAFS spectra of multilayer formic acid condensed on Si(1 1 1) [7] are compared to the C1*s* and O1*s* ISEEL spectra of HCOOH in Fig. 5. NEXAFS spectra recorded with both 20 and 90° incidence angles are plotted. Although the majority of the gas phase C1*s* and O1*s* spectral features are also seen (at considerably lower resolution) in the multilayer NEXAFS, the second peak in the gas phase O1*s* ISEELS does not appear to have a counterpart in the O1*s* NEXAFS of the multilayer. Exactly the same change in the O1*s* spectrum is found when the gas and multilayer O1*s* spectra of the other three carboxylic acids are compared (compare Fig. 4 of this work with Fig. 5 of ref. 7). The O1*s* → π^*(C=O) transition occurs at 533(1) eV with a FWHM of 4.0(5) eV in the NEXAFS of all four acids. The π^* peaks in the O1*s* NEXAFS of formic and propiolic acid are discernably asymmetric with high energy tails. In comparison, the two strong discrete lines in the O1*s* ISEELS occur at 532.0(3) eV and 535.2(3) eV (the number in brackets giving the range of values observed for the four acids).

Except for the layer adjacent to the Si(1 1 1) surface, the multilayer acids are believed to closely resemble the bulk solid. All carboxylic acids are dimerized in the solid state. By contrast, the acids are in predominantly monomer form under the low pressures ($< 10^{-4}$ torr) of the sample chamber of the ISEEL spectrometer if the monomer/dimer equilibrium [32] is established. This is believed to be the case because of a long (ca. 1 m), convoluted, low pressure path length between the sample inlet and the collision cell in our spectrometer. Increasing this path length to 4 m [5] caused no detectible change in the O1*s* spectrum of formic acid, supporting our conclusion that equilibrium is established and that the monomer predominates under our normal spectrometer conditions.

The structure of the carboxyl group in the condensed phase is expected to be similar to that reported for the dimer of formic acid [30] (see Fig. 5). There is relatively little change in either the C=O or the C—OH bond lengths and thus

we expect relatively small changes in the 1*s* IPs or the π^*(C=O) energy between the monomer and the dimer. This is supported by the small shift in the p(C=O) IP which is 15.76 eV in the monomer and 15.3, 15.7 eV in the dimer [29]. Based on the small geometry change, a reasonably large O1*s*(C=O)—O1*s*(OH) chemical shift might be expected to persist in the dimer, thus one would expect a second discrete peak to appear in the multilayer NEXAFS corresponding to that observed in the gas phase ISEELS. However, there was no obvious sign of it. We emphasize that this experimental observation is independent of the assignment of the second peak. There are several possible explanations for the difference between the gas and multilayer spectra. We will consider the merits and limitations of each in turn.

One explanation is that a second discrete transition does exist in the multilayer but is not resolved from the O1*s*(C=O) $\rightarrow$ π^*(C=O) transition due to a combination of lower NEXAFS resolution (> 1.5 eV as opposed to 0.6 eV in ISEELS) along with energy shifts associated, in part, with some decrease in the separation of the C=O and OH O1*s* IPS on dimerization. This suggestion is supported both by shifts ranging from 0.7 to 1.3 eV between the first peak in the gas phase O1*s* spectrum and that in the multilayer NEXAFS, and by the large breadth (4.0 eV FWHM) of the π^*(C=O) resonance in the O1*s* NEXAFS spectra [7]. This interpretation is also supported by recent higher resolution measurements of the O1*s* NEXAFS of multilayer HCOOH on W(100)(5 × 1)C [33] in which a distinct shoulder was observed at 534.0 eV, 1.7 eV above the main π^*(C=O) peak at 532.3 eV. Although the possibility of spectral modifications due to the different substrates must be considered, these results appear to be consistent with those of Outka et al. [7] for carboxylic acids on Si(111), taking into account the considerably lower resolution in their experiment. When least squares curve fits are performed on the first structure in the O1*s* 20° NEXAFS spectrum of formic acid on Si(111), an excellent match to two gaussian peaks with a separation of 1.7(1) eV is found. This separation is considerably smaller than that of the first two peaks in the gas phase carboxylic acid spectra (3.2–3.7 eV) but is identical to that observed in the O1*s* NEXAFS of formic acid multilayers on W(100) – (5 × 1)C [33]. However, we note that a single gaussian lineshape along with an underlying "atomic continuum" contribution was found to provide an equally satisfactory fit to the Si(100) multilayer HCOOH data [34].

If the two peaks were coalesced one would expect the intensity to be preserved. When the NEXAFS data are converted to approximate oscillator strengths through continuum normalization to atomic calculations [16], the O1*s* $\rightarrow$ π^*(C=O) oscillator strength is 0.063 in the multilayer 20° NEXAFS, as compared to 0.057 for the sum of the two π^*(C=O) peaks in the gas phase O1*s* ISEELS of formic acid. In the NEXAFS of all four carboxylic acids the π^* resonances are most intense at glancing incidence. Because of the polarization dependence, O1*s* $\rightarrow$ π^* transitions in molecules lying parallel to the surface should be more intense in the 20° incidence geometry that in the case of random orientation in the gas phase. Thus the somewhat greater intensity in the 20° NEXAFS is consistent with both gas phase (monomer) transitions being

present but unresolved in the solid (dimer). The quantitative comparison suggests a somewhat reduced intensity of the second component.

Within the context of our preferred assignment of predominantly O1*s*(OH) → π^*(C=O) transitions for the second peak in the gas phase, a decrease in the O1*s*(OH) → π^*(C=O) charge transfer transition intensity in the multilayer could explain this reduced intensity. If this charge transfer transition arises because of a gross distortion of the π^* orbital due to relaxation towards the core hole, as has been suggested for the HCOX species [5], the presence of the Si(111) surface and other nearby molecules (such as the other RCOOH molecule of the dimer) could have a large influence on the O1*s*(OH) core hole relaxation. This could lead to a drop in the intensity of the O1*s*(OH) → π^*(C=O) transition between the gas and the multilayer. Alternatively, if one adopts an O1*s*(OH) → σ^*(O—H) assignment for the second peak in the gas phase ISEELS, the energy shift, and presumably the reduced intensity, could be related to the relatively large (6%) increase in the O—H bond length between the monomer (0.97 Å) and the dimer (1.03 Å) [30].

Another possibility is that the majority of the carboxylic acids are deprotonated in the condensed phase. This is known to occur in monolayers on certain substrates [2, 24, 35] and could be an essentially quantitative process even in multilayers by O—H bond breaking and Si—H bond formation if the multilayer was not too thick. In the resulting carboxylate species the two C—O bonds would most likely be equivalent and thus only one O1*s* → π^*(C=O) feature would be expected, as has been observed in the O1*s* NEXAFS of formate on two copper surfaces [24, 35–37]. However, two points argue strongly against this explanation. Firstly, in the NEXAFS studies of formate on metal surfaces the O1*s* → π^* transition occurs at 535 eV, more than 2 eV higher than the O1*s* NEXAFS peak of the multilayer acids. Secondly, the O1*s* NEXAFS of monolayer propiolic acid on Si(111) does not exhibit any strong polarization dependence (in contrast to the multilayer) whereas the $RCOO^-$ structure would be expected to be strongly, and probably symmetrically, attached to the surface, so that a definite orientation of the π and σ systems relative to the surface would be achieved. Thus, for instance, the NEXAFS spectrum of monolayer formic acid on Cu(100) (where all evidence is consistent with a formate, $HCOO^-$ structure [24, 35–37]) shows only a single O1*s* → π^*(C=O) feature (535 eV, FWHM = 4.0 eV) which has a very strong polarization dependence. A shift in the O1*s* → π^*(C=O) resonance between 533 and 535 eV appears to be characteristic of the conversion between acid and carboxylate structures.

In summary, it would appear that the difference between the O1*s* spectra of the gas and the multilayer arises from a combination of reduced resolution along with spectral changes related to the dimerization of the acids in the condensed phase. The magnitude of the spectral changes with dimerization could be most directly determined by obtaining the spectrum of the dimer in the gas phase. To date, all ISEELS studies of formic acid using a more direct inlet line and higher pressures (with estimated collision cell pressures of up to

4×10^{-3} torr and an equilibrium dimer concentration of ca. 10% [32]) have not produced any observable changes in the second O1*s* peak.

Methyl formate

The oscillator strength spectra of HCOOH, $HCOOCH_3$ and CH_3OH are shown in Figs. 6 (C1*s*) and 7 (O1*s*). Our spectra of CH_3OH are in good agreement with earlier work [6] with regard to energies and relative intensities. The energies, term values and proposed assignments for the $HCOOCH_3$ spectral features are summarized in Table 7 and compared with those of HCOOH and MeOH. This comparison allows a further test of the chromophore concept and thus the additivity of inner-shell excitation spectral features. In order to carry this idea to its logical limits we have compared sums of the HCOOH and CH_3OH spectra to the C1*s* and O1*s* spectra of methyl formate in Fig. 8. For the C1*s* comparison a simple sum was used. The weightings of 0.9 (HCOOH) and 0.2 (CH_3OH) used to simulate the O1*s* spectrum were chosen both to correct for the differing number of oxygens and to produce good agreement in the non-resonant continuum and at the π^* peak.

Overall there is excellent agreement of both peak energies and intensities for C1*s* excitation. In particular, the C1*s* → π^*(C=O) peak in methyl formate has an oscillator strength (0.063) which is close to the sum of the C1*s* → π^*(C=O) intensity in HCOOH (0.056) and the C1*s* → 3*s* intensity in CH_3OH (0.012). The second peak in methyl formate corresponds to the C1*s*(CH_3) → 3*p*/π^*(C—H) transition in methanol. The third, fourth and fifth peaks are predominantly C1*s*(HC) → Ryd/σ^*(HCO) excitations corresponding to the Rydberg structure in formic acid, but there is also underlying intensity from the C1*s* → σ^*(C—O) transition. The broad continuum maxima 6 and 7 in the $HCOOCH_3$ spectrum match those for formic acid and are similarly assigned to the σ^*(C—O) and σ^*(C=O) resonances.

In the case of O1*s* excitation there is generally good agreement between the spectrum of methyl formate and the weighted sum of those of formic acid and methanol (Fig. 8). The differences that exist are exactly those expected from the replacement of the O—H bonds in methanol and formic acid by a C—O bond. In particular, we expect that features arising from O1*s* → σ^*(O—H) in formic acid and methanol will disappear while additional O1*s* → σ^*(C—O) intensity will be introduced. In addition, some displacement of transitions will occur due to chemical shifts of the O1*s* orbital energies, although the term values are expected to correspond. The absolute energy of the O1*s*(C=O) → π^*(C=O) peak matches that of formic acid since the O1*s*(C=O) IP is not greatly shifted. The second peak in the methyl formate spectrum matches that for formic acid (attributed to overlapping O1*s*(OH) → π^*(C=O) and O1*s*(C=O) → 3*s*/σ^*(HCO) transitions [5]) although it is much weaker. The O1*s*(OH) → π^*(C=O) charge transfer transition may be reduced in intensity because the O1*s*(OCH_3) core hole can be shielded more efficiently by the greater electron density of the CH_3 group in methyl formate than by the single hydrogen in formic acid and thus

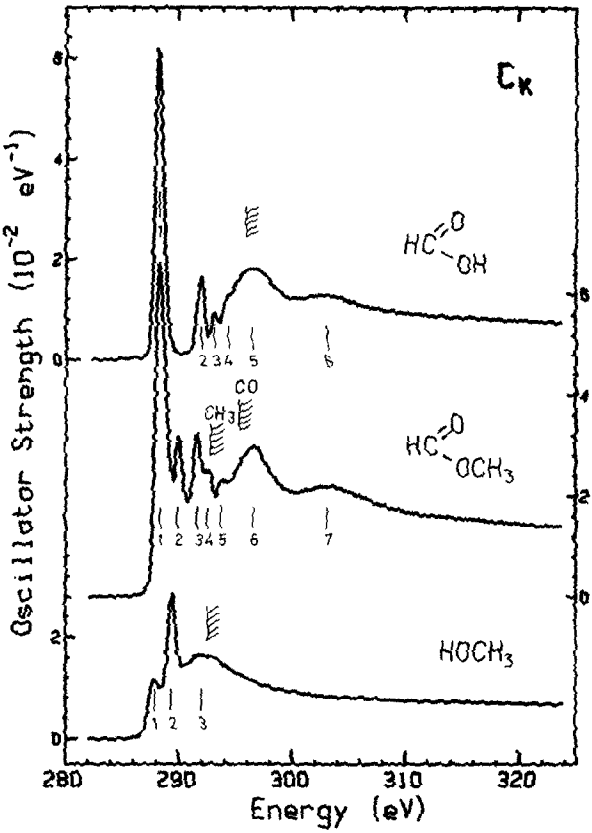

Fig. 6. Oscillator strengths for C1s excitation of formic acid, methyl formate and methanol, derived from ISEELS. See caption to Fig. 1 for further details.

there is less distortion of the π^*(C=O) orbital towards the O*CH_3 core hole. Alternatively, the decreased intensity of feature 2 in the methyl formate spectrum as compared to its counterpart for formic acid could indicate that this feature contains significant contributions from O1s(OH) → σ^*(O—H) transitions. As noted earlier, the term value of the second feature relative to the O1s(OH) IP (5.4–5.9 eV for the acids) is as close to the O1s → σ^*(O–H) term values for the alcohols (4.6–4.9 eV) as those of the third feature in the acid spectra (3.1–3.3 eV), which we have assigned to σ^*(O—H) in Tables 4–6. Feature 3 at 537.6 eV for formic acid is also absent in the methyl formate spectrum, which is consistent with its assignment to σ^*(O—H) for the acids. If the alternate O1s → σ^*(O—H) assignment is adopted for feature 2 for the acids, then its apparent absence in the multilayer NEXAFS would indicate extensive deprotonation. Outka et al. [7] do not believe that this deprotonation has occurred and the absence of any shift of the π^*(C=O) resonance to higher energy as expected in the postulated carboxylate gives support to this.

TABLE 7

Absolute energies, term values and proposed assignments for features in the C1*s* and O1*s* spectra of methyl formate compared to those of methanol and formic acid

Carbon 1*s*

$HCOOCH_3$						CH_3OH			HCOOH[a]		
Feature	Energy (eV)	Term value (eV)		Assignment		Feature	*E*	*T*	Feature	*E*	*T*
		T_{CH_3}	T_{HC}	CH_3	HC						
1	288.3[b]	4.4	6.8	3*s*	π^*(C=O)	1	287.9	4.5	1	288.2	7.6
2	290.0	2.8	–	$\pi^*(CH_3)$	–	2	289.4	3.0		–	
3	291.6	–	3.5	–	σ^*(HCO)		–		2	292.0	3.8
IP(CH_3)	292.78[c]					IP	292.4				
4	292.6	–	2.5	–	3*p*		–		3	293.2	2.6
5	293.7	−0.9	–	σ^*(C—O)	–	3	292.4	0	4	294.2	1.6
IP(HC)	295.14[c]								IP	295.8	
6	296.6	–	−1.5	–	σ^*(C—O)		–		5	296.1	−0.3
7	303(2)	–	−8	–	σ^*(C=O)		–		6	303(1)	−7

Oxygen 1*s*

$HCOOCH_3$						CH_3OH			HCOOH		
Feature	Energy (eV)	Term value (eV)		Assignment		Feature	*E*	*T*	Feature	*E*	*T*
		$T_{C=O}$	T_{OCH_3}	C=O	OCH_3						
1	532.1[b]	6.4	–	π^*(C=O)	–		–		1	532.1	6.9
2	535.1	3.4	4.8	3*p*/σ^*(HCO)	π^*(C=O)	1	534.1	5.0	2	535.3	3.7/5.4
3	536.9	–	3.0	–	σ^*(C—O)	2	537.3	1.8	3	537.6	1.4
IP(C=O)	538.5[c]								IP	539.0	
4	539.8	–	0.1		Ryd		–				
IP(OCH_3)	539.9[c]					IP	539.1		IP	540.7	
5	541(1)	−1.5	–	σ^*(C—O)	–		–		4	542.1	−1.4
6	547(1)	−9	–	σ^*(C=O)	–		–		5	547(1)	−8

[a] From [5]. Note that the feature numbering differs slightly to the previous tables. The numbers listed here correspond to those on Figs. 6 and 7.
[b] Calibration: C1*s*, 2.42(5) eV below ($C1s^{-1}$, π^*) of CO_2; O1*s*, 3.28(5) eV below ($O1s^{-1}$, π^*) of CO_2. [c] IPs from XPS [18].

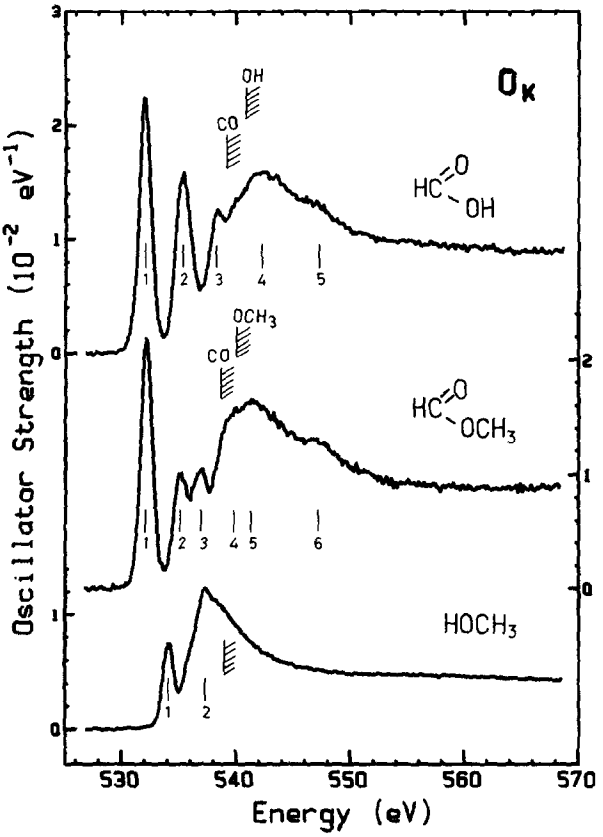

Fig. 7. Oscillator strengths for O1*s* excitation of formic acid, methyl formate and methanol, derived from ISEELS. See caption to Fig. 1 for further details.

Although it appears to be considerably sharper, peak 3 in the O1*s* spectrum of methyl formate is a good match in energy (but not term value) to the O1*s* → σ^*(C—O) resonance in methanol and is thus similarly assigned. The decreased width of the O1*s* → σ^*(C—O) transition is consistent with its greater term value (which correlates [4] with a longer O—C bond in methyl formate (R_{C-O} = 1.437 Å) than in methanol (R_{C-O} = 1.425 Å) [30]). To some extent the apparent sharpness is also due to the onset of the O1s(OCH_3) continuum and the higher energy features 4, 5 and 6, which are attributed to unresolved O1*s*(OCH_3) → Rydberg, O1*s*(C=O) → σ^*(C—O) and O1*s*(C=O) → σ^*(C=O) transitions, respectively. The poor agreement in the region of feature 3 between the O1*s* spectrum of methyl formate and our simulation based on (0.9HCOOH + 0.2CH_3OH) can be improved by increasing the CH_3OH component in the simulation. Overall the methyl formate spectra can be interpreted very satisfactorily as the sum of localized inner-shell excitations to

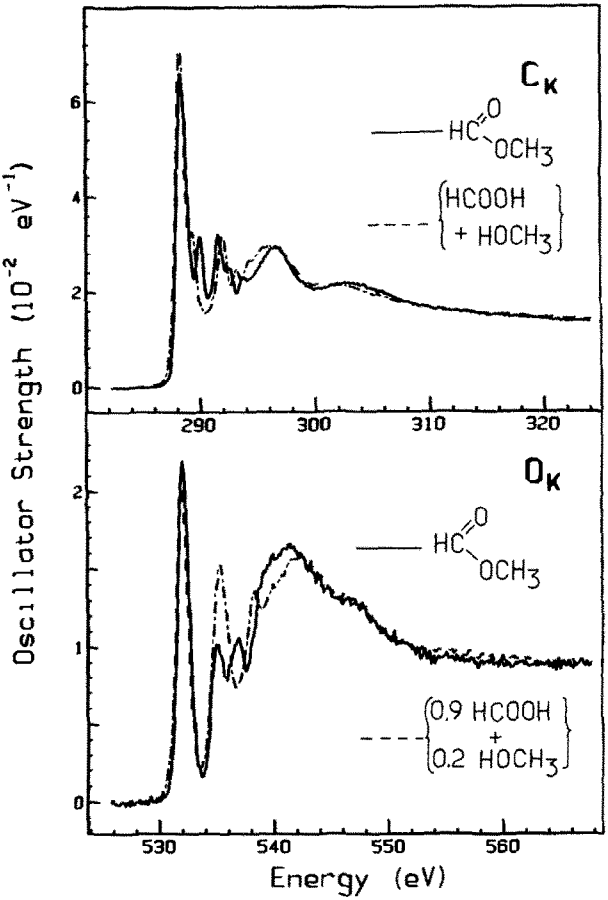

Fig. 8. Comparison of the C1*s* and O1*s* oscillator strength spectra of methyl formate with the indicated weighted sums of the corresponding spectra of formic acid and methanol. The energy scales were not shifted prior to addition.

unoccupied orbitals characteristic of the molecular chromophores. A similar approach has been used previously to interpret the spectrum of CH_3CH_2Cl in terms of the sum of the spectra of ethane and methyl chloride [38].

Trends in π^* term values and oscillator strengths

1s → π^*(C=O) excitation

The term values and oscillator strengths of 1*s* → π^*(C=O) transitions in a variety of molecules are presented in Table 8. In general, excitations to π^*(C=O) from the carbonyl C1*s* and O1*s* have very similar term values. The greatest difference (1.1 eV) is found in propiolic acid, presumably because the conjugation between π^*(C≡C) and π^*(C=O) is greater with a C1*s* than an O1*s*

TABLE 8

Term values and oscillator strengths of $1s \rightarrow \pi^*(C{=}O)$ transitions of organic acids and esters

Molecule	Term values (eV)			Oscillator strength ($f \times 10^{-2}$)		
	C1*s*	O1*s*(C=O)	O1*s*(OH)[a]	C1*s*	O1*s*(C=O)	O1*s*(OH)[a]
$HCOOCH_3$	6.8	6.4	4.8	6.3	2.7	(1.5)[b]
HCOOH	7.6	6.9	5.4	5.6	2.9	2.8
CH_3CH_2COOH	7.0	7.1	5.6	10.0	2.3	2.6
$CH_2{=}CHCOOH$	7.3	7.7	5.9	7.7	2.1	3.0
$HC{\equiv}CCOOH$	6.6	7.7	5.8	8.2	2.3	3.6

[a] The O1*s*(O—H) designation also refers to O1*s*(OCH_3) in methyl formate.
[b] Part of the intensity of this transition is believed to arise from O1*s*(C=O) → Ryd and/or O1*s*(O—H) → σ^*(O—H) excitations.

hole. The term values for the features assigned to O1*s*(OH) → π^*(C=O) excitation are 1.5–2.0 eV smaller than O1*s*(C=O) → π^*(C=O) or C1*s*(C=O) → π^*(C=O) excitations. This decrease in the term value can be considered as an energy penalty associated with the unfavorable charge transfer [22] from the O1*s*(O—H) absorption site to the π^*(C=O) which is localized on the carbonyl. The magnitude of this shift indicates that the π^*(C=O) orbital delocalizes only slightly onto the hydroxyl oxygen. In addition, the greater intensity of the O1*s*(C=O) → π^*(C=O) compared with the O1*s*(O—H) → π^*(C=O) transition is consistent with the π^*(C=O) orbital being concentrated on the carbonyl group. The C1*s* → π^*(C=O) intensity is consistently 2–4 times greater than the O1*s* → π^* intensity, indicating that the π^*(C=O) orbital has greater density on the carbon than the oxygen atom. The same result was found in our earlier study of formamide, formic acid and formyl fluoride [5].

TABLE 9

Term values and oscillator strengths of C1*s* → π^*(C≡C) and C1*s* → π^*(C=C) transitions

Alkynes	π^*(C≡C)		Alkenes	π^*(C=C)	
Molecule	*T*	($f \times 10^{-2}$)	Molecule	*T*	($f \times 10^{-2}$)
$HC{\equiv}CH$[a]	5.2	14.3	$CH_2{=}CH_2$[a]	6.3	6.8
$CH_3C{\equiv}CH$[b]	5.1	14.4	$CH_3CH{=}CHCH_3$[c]	5.8	7.5[d]
$CH_3C{\equiv}CCH_3$[e]	5.1	14.4	$CH_2{=}CHCH_2CH_3$[c]	5.7	7.5
$HC{\equiv}CCH_2OH$	5.4	12.2	$CH_2{=}CHCH_2OH$	6.2	6.6
$HC{\equiv}CCOOH$ (π^*)	5.1, 6.1	7.8	$CH_2{=}CHCOOH$	6.7, 7.2	5.5
($\pi^{*\prime}$)	6.1, 6.6	3.6			

[a] From ref. 13. [b] Unpublished spectrum [21]. [c] From ref. 11. [d] Average of *cis* (7.0) and *trans* (8.1) π^*_{osc} strengths (analysis of data reported in ref. 15). [e] From ref. 22.

1s → π(C=C) excitations*

The term values and oscillator strengths of 1s → π*(C=C) and 1s → π*(C≡C) transitions in a variety of molecules are presented in Table 9. In the absence of π-conjugation, the term values of both transitions are remarkably constant, with values of 5.2(2) eV for π*(C≡C) and 5.9(3) eV for π*(C=C). As discussed previously the splitting of the π*(C≡C) peak in propiolic acid arises from conjugation with the π*(C=O) orbital. It is clear from the term values that the lower energy peak corresponds to π*′(C≡C), the component conjugated with π*(C=O). The term value of the C1s → π*(C=C) transition in CH_2=CHCOOH appears to be about 0.5 eV higher than the corresponding C1s → π*(C=C) term values in CH_2=CH_2 and CH_2=$CHCH_2OH$. Note that we attach an uncertainty of 0.3–0.5 eV to our estimated IPs and thus this difference may fall within the margin of error. If this is not the case, the increased term value of the C1s → π*(C=C) transition could result from partial conjugation between the π*(C=C) and π*(C=O) levels in acrylic acid. Such interactions would be expected to occur in a planar conformation. The decreased shift for acrylic acid, as compared to the shift in the π*′(C≡C) term value of propiolic acid relative to propargyl alcohol, would then be consistent with the contributions of the non-planar conformations of acrylic acid, which do not exist in the rigidly planar propiolic acid.

The oscillator strengths of the C1s → π* transitions are also very constant, having values of 0.06–0.08 in the alkenes and 0.12–0.14 in the alkynes. Again this constancy is disturbed by π-conjugation. Neither of the C1s → π*(C≡C) transitions in propiolic acid is as intense as the C1s(CH_x) → π*(C≡C) transition in propargyl alcohol and even the sum of the two is somewhat less (see Table 9). The decreased C1s → π* intensity is consistent with the partial π*(C=O) character of the π*′(C≡C) orbital since the C1s → π*(C=O) transition is always weaker than the C1s → π*(C=O) transition. The low intensity of the C1s → π*′(C≡C) compared with the C1s → π*(C≡C) transition is consistent with this shared character. Also, it indicates that the electron distribution in the π*′(C≡C) orbital is reduced at the (CH) and (—C≡C) carbons relative to that in π*(C≡C) and is displaced overall towards the carbonyl group.

SUMMARY

The oscillator strength spectra of methanol, three C_3-carboxylic acids, three C_3 alcohols and methyl formate in the regions of C1s and O1s excitation have been derived from electron energy loss spectra recorded under dipole conditions. These spectra have been analyzed in comparison with the NEXAFS of their multilayer counterparts. The remarkable similarity of the gas and condensed phase spectra indicates that the geometric and electronic structure of these molecules is relatively undistorted in the multilayer, an assumption underlying the NEXAFS interpretation [7]. A dramatic exception to this

generalization is found in O1*s* excitation of the carboxylic acids where in each of the 4 cases studied to date there is a reduction in the number of sharp, low energy resonances from 2 to 1, which we have attributed to O1*s* → π^*(C=O) transitions. A measurement of the O1*s* spectrum of a gas phase carboxylic acid dimer would determine whether this difference is connected solely with the expected dimerization in the condensed phase or whether an additional mechanism is operative. The O1*s* and particularly the C1*s* spectra of methyl formate are found to be in excellent agreement with the sum of the spectra of formic acid and methanol, further supporting the interpretation of inner-shell excitation spectra in terms of localized excitations to unoccupied π^* and σ^* orbitals characteristic of the chromophores present in the molecule.

ACKNOWLEDGMENTS

This research was financially supported by IBM (San Jose) and by NSERC (Canada). Fruitful discussions with Dr. J. Stöhr are acknowledged. We thank Dr. C. Friend for sending her results prior to publication. APH thanks NSERC for financial support in the form of a university research fellowship. He also thanks the staff of Laboratoire LURE for their hospitality during the period in which this was written.

REFERENCES

1 C.E. Brion, S. Daviel, R.N.S. Sodhi and A.P. Hitchcock, AIP Conf. Proc. 94 (1982) 426.
2 J. Stöhr, Z. Phys. B, 61 (1985) 439; J. Stöhr, in R. Vaneslow and R. Howe (Eds.), Chemistry and Physics of Solid Surfaces Vol. V, Springer, Berlin, 1984, p. 231; J. Stöhr, in D. Konigsberger and R. Prins (Eds.), X-Ray Absorption: Principles, Applications, Techniques of EXAFS, SEXAFS and XANES, Wiley, New York, 1986.
3 A.P. Hitchcock, J. Electron Spectrosc. Relat. Phenom., 25 (1982) 245. (Updated versions of this bibliography of inner-shell excitation studies of gaseous atoms and molecules are available from the author.)
4 F. Sette, J. Stöhr and A.P. Hitchcock, J. Chem. Phys., 81 (1984) 4906.
5 I. Ishii and A.P. Hitchcock, J. Chem. Phys., 87 (1987) 830.
6 G.R. Wight and C.E. Brion, J. Electron Spectrosc. Relat. Phenom., 4 (1974) 25.
7 D.A. Outka, J. Stöhr, R.J. Madix, H.H. Rotermund, B. Hermsmeier and J. Solomon, Surf. Sci., 185 (1987) 53.
8 J.A. Horsley, J. Stöhr, A.P. Hitchcock, D.C. Newbury, A.L. Johnson and F. Sette, J. Chem. Phys., 83 (1985) 6099.
9 A.P. Hitchcock, D.C. Newbury, I. Ishii, J. Stöhr, J.A. Horsley, R.D. Redwing, A.L. Johnson and F. Sette, J. Chem. Phys., 85 (1986) 4849.
10 A.P. Hitchcock, J.A. Horsley and J. Stöhr, J. Chem. Phys., 85 (1986) 4835.
11 D.C. Newbury, I. Ishii and A.P. Hitchcock, Can. J. Chem., 64 (1986) 1145.
12 G. Tourillon, S. Ragen, T.A. Skotheim, M. Sagurton, R. Garrett and G.P. Williams, Surf. Sci., 184 (1987) L345.
13 A.P. Hitchcock and C.E. Brion, J. Electron Spectrosc. Relat. Phenom., 10 (1977) 317.
14 D. Arvanitis, U. Döbler, L. Wenzel, K. Baberschke and J. Stöhr, Surf. Sci., 178 (1986) 687; D. Arvanitis, K. Baberschke, L. Wenzel and U. Döbler, Phys. Rev. Lett., 57 (1986) 3175.
15 A.P. Hitchcock, S. Beaulieu, T. Steel, J. Stöhr and F. Sette, J. Chem. Phys., 80 (1984) 3927.
16 G. Doolan and D. Liberman, Phys. Scr., (1987) in press.

17 R. McLaren, S.A.C. Clark, I. Ishii and A.P. Hitchcock, Phys. Rev. A, 36 (1987) 1683.
18 W.L. Jolly, K.D. Bomben and C.J. Eyerrmann, At. Data Nucl. Data Tables, 31 (1984) 433.
19 A.P. Hitchcock and I. Ishii, J. Electron Spectrosc. Relat. Phenom., 42 (1987) 11.
20 D. Arvanitis, J. Stöhr, K. Baberschke and J.A. Horsley, Phys. Rev. B, 36 (1987) 2976.
21 I. Ishii and A.P. Hitchcock, unpublished work.
22 M.B. Robin, I. Ishii, R. McLaren and A.P. Hitchcock, J. Electron Spectrosc. Relat. Phenom., in press.
23 I. Ishii, R. McLaren, A.P. Hitchcock and M.B. Robin, J. Chem. Phys., (1987) in press.
24 J. Stöhr, J.L. Gland, W. Eberhardt, D. Outka, R.J. Madix, F. Sette, R.J. Koestner and U. Döbler, Phys. Rev. Lett., 51 (1983) 2414; D. Outka, R.J. Madix and J. Stöhr, Surf. Sci., 164 (1985) 235.
25 M. Bader, A. Puschmann and J. Haase, Phys. Rev. B: 33 (1986) 7336.
26 M.D. Crapper, D.P. Woodruff, M. Bader and J. Haase, Surf. Sci., 182 (1987) L241.
27 A. Barth, R.J. Buenker, S.D. Peyerimhoff and W. Butscher, Chem. Phys., 46 (1980) 149.
28 D. Klapstein, J. Electron Spectrosc. Relat. Phenom., 42 (1987) 149.
29 K. Kimura, S. Katsumata, Y. Achiba, T. Yamazaki and S. Iwata, Handbook of He I Photoelectron Spectra of Fundamental Organic Molecules Halsted, New York, 1981.
30 Structure Data of Free Polyatomic Molecules, Vol. 7, Landolt-Bornstein, New Series II, Springer, Berlin, 1976.
31 A.P. Hitchcock and C.E. Brion, J. Electron Spectrosc. Relat. Phenom., 19 (1980) 231.
32 W. Waring, Chem. Rev., 51 (1952) 171.
33 C. Friend, private communication, 1986.
34 D. Outka and J. Stöhr, private communication.
35 M.D. Crapper, C.E. Riley, D.P. Woodruff, A. Puschmann and J. Haase, Surf. Sci., 171 (1986) 1.
36 M.D. Crapper, C.E. Riley and D.P. Woodruff, Surf. Sci., 184 (1987) 121.
37 J. Stohr, D. Outka, R.J. Madix and U. Doblër, Phys. Rev. Lett., 54 (1985) 1256.
38 A.P. Hitchcock and C.E. Brion, J. Electron Spectrosc. Relat. Phenom., 14 (1980) 417.
39 A.P. Hitchcock and C.E. Brion, J. Electron Spectrosc. Relat. Phenom., 13 (1980) 1.
40 R.N.S. Sodhi and C.E. Brion, J. Electron Spectrosc. Relat. Phenom., 34 (1984) 363.
41 G.R. Wight and C.E. Brion, J. Electron Spectrosc. Relat. Phenom., 4 (1974) 313.